BOLETIN DE LA SOCIEDAD ESPAÑOLA DE
Cerámica y Vidrio
www.elsevier.es/bsecv

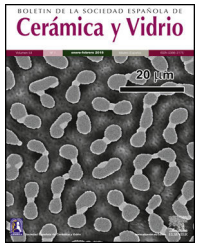

Down conversion and efficient NIR to visible up-conversion emission analysis in Ho^{3+}/Yb^{3+} co-doped tellurite glasses

Sharafudeen Kaniyarakkal[a,*], *Kesavulu Culala Rajasekharaudayar*[b], *Rajesh Dagupati*[c], *Yang Li*[d], *Zhi Chen*[e], *Vijayakumar Sadasivan Nair*[f], *Shiju Edappadikkunnummal*[g]

[a] *Department of Physics, Kuwait College of Science and Technology, Doha 35004, Al-Asimah, Kuwait*
[b] *Department of Physics, Institute of Aeronautical Engineering (IARE), Hyderabad 500043, India*
[c] *FunGlass, Alexander Dubcek University of Trencin, Studentska 2, SK-911 50 Trencin, Slovakia*
[d] *Department of Biomedical Engineering, Guangzhou Medical University, Guangzhou 510180, China*
[e] *Zhejiang Lab, Hangzhou 311100, China*
[f] *PG and Research Department of Physics, N S S College Pandalam, Pathanamthitta 689501, Kerala, India*
[g] *Physics Division, School of Advanced Sciences and Languages, VIT Bhopal University, Madhya Pradesh, 466114, India*

ARTICLE INFO

Article history:
Received 8 September 2022
Accepted 9 January 2023
Available online 30 January 2023

Keywords:
NIR light
Rare earth
Synthesis
Up-conversion

ABSTRACT

A series of glasses with chemical composition (50−*x*−*y*) TeO_2–30ZnO–10YF_3–10NaF–xHo_2O_3–yYb_2O_3 (*x* = 0.5 and *y* = 0.5, 1.0, 3.0, 5.0 mol%) were prepared by melt-quenching procedure. The absorption spectra, excitation, down conversion emission spectra, up-conversion (UC) emission spectra and decay time measurements were analyzed. In down conversion, the visible emission transition intensity associated with $^5F_4 \rightarrow {}^5I_8$ (547 nm), $^5F_5 \rightarrow {}^5I_8$ (657 nm), and $^5F_4 \rightarrow {}^5I_7$ (755 nm) of Ho^{3+} ions decreased with Yb^{3+} concentration due to the energy transfer (ET) process from Ho^{3+} to Yb^{3+} ions. In up-conversion, on exciting with 980 nm diode laser beam, we observed a strong green (543 nm) and red (657 nm) UC emissions, that refers to the energy level transitions; $^5F_4$ ($^5S_2$) $\rightarrow {}^5I_8$ and $^5F_5 \rightarrow {}^5I_8$ of Ho^{3+}. The influence of excitation power on UC intensities studies revealed that the population at $^5F_4$ ($^5S_2$) and $^5F_5$ levels of Ho^{3+} ion occurs due to two-photon absorption process associated energy transfer from Yb^{3+} to Ho^{3+}. The influence of Yb^{3+} doped concentration on UC was studied, and it is observed that both the green and red UC intensities improved significantly on increasing Yb^{3+} ions concentration.

Introduction

The lasers operating in the visible region of electromagnetic spectrum have been employed for a number of applications like optical recording, display, medical diagnosis, etc. [1]. Energy-up conversion (UC) property of rare earth (RE) ions are an efficient way to obtain visible lase under IR pumping. Besides the visible laser, material exhibiting UC luminescence have also getting special consideration due to their potential use for IR sensing, in photovoltaics as solar NIR concentrators, and biological classification [2,3]. It is essential to understand

* *Corresponding author.*
E-mail address: s.valappil@kcst.edu.kw (S. Kaniyarakkal).
https://doi.org/10.1016/j.bsecv.2023.01.002

the exact mechanism, in order to exploit a competent up-converting material and to enhance their efficiency.

A number of studies were reported on tellurite glasses during the last few years owing to its attractive attributes. It is transparent for a wide range of wavelengths (0.35–5 μm) in comparison to silicate glasses (0.2–3 μm), and has large index of refraction [4,5]. It also has excellent stability, and lower phonon energy. Among the number of RE ions available, Ho^{3+} has exceptional UC luminescence due to its apparent transitions which spans in the visible region [6,7]. Even though, Ho^{3+} is an excellent candidate, it has some draw backs, like one cannot directly excite it with commercially available diode laser (LD), 980 nm because of the absence of appropriate absorption levels in it. Fortunately, co-doping with Yb^{3+} enables sensitization of Ho^{3+} to realize visible UC transition due to the accessibility of its large absorption cross-section about 980 nm [8,9] in addition to its efficient energy transfer ability to Ho^{3+} [9,10]. Ho^{3+} can be employed into matrixes as activators to initiate interesting luminescent mechanisms. Due to their rich energy level occurrence, the emissions in red, green and many other wavelengths can occur under IR laser excitations for ex. 980 nm wavelength. With Ho^{3+}, Yb^{3+} addition as a sensitizer and a co-dopant can bring improved up-conversion emissions [11,12]. Balaji et al. have analyzed phonon assisted energy transfer process in Ho^{3+}/Yb^{3+} co-doped telluride glass, and found that in order to achieve a substantial energy transfer the difference in energy between $^2F_{5/2}$ (Yb^{3+}) and $^5I_6$ (Ho^{3+}) levels can be crossed with the aid of host phonons [13]. It can be noted that because of the non-resonant transitions the Yb^{3+} emission and Ho^{3+} absorption has a very poor spectral overlap of about 1500 cm^{-1} energy gap. Since the telluride glasses have a ~750 cm^{-1} of phonon energy, nearly two or three phonons are needed to cross the transition gap in energy. On the contrary, the host systems that have high phonon energy like phosphate, silicate, and borate can achieve this energy gap bridging with a smaller number of phonons, but non radiative transition from $^5I_7$ level of Ho^{3+} restricts the 2 μm emission probabilities significantly. Their study also estimated the energy transfer microparameters to be reasonably good magnitude, which substantiates that the ET process benefits from host phonons. Thus, the telluride glass is promising host for Ho^{3+}/Yb^{3+} co-doping for efficient NIR emissions and up-conversions. For the last few years, numerous research works were conducted on Yb^{3+}/Ho^{3+} doped tellurite glasses for the advance of solid-state UC green emitting lasers, mid-infrared optical fiber amplifiers and laser devices [11–16]. The studies reported by Wang et al., have shown enhanced luminescent properties via tailoring the phonon energy and crystal fields' environment in Ho^{3+}/Yb^{3+} based silicate system [17]. Le et al. reported Ho^{3+}/Yb^{3+} in tellurite glasses with enhanced up-conversion NIR emissions [18]. Suresh et al. [19] studied $Ho^{3+/}Yb^{3+}$ co-doped zinc tellurite glasses that exhibit blue-green photon into NIR photons transitions and it is found useful for solar conversion and optical amplifier applications. Zhu et al. [20] presented the emission improvement in the 2.0 μm band and effective energy transfer process in $Ho^{3+}/Yb^{3+}/Er^{3+}$ tri-doped tellurite glasses for solid state laser applications. Guangning et al. [21] depicted the mid-infrared 2.0 μm and 4.1 μm wideband emission in Ho^{3+}/Yb^{3+} doped tellurite–germanate glasses that are suitable for mid-infrared fiber and laser materials applications. Azam et al. [22] explained the photo luminescence studies with Judd–Ofelt analysis in Ho^{3+}/Ho^{3+}–Yb^{3+} doped/co-doped lead tellurite glasses for use in optical multi-functional devices. Chao et al. [23] discussed enhancement in UC and 2 μm mid-infrared emission in Ho^{3+}/Yb^{3+} co-dopped tellurite glass for UC and mid-infrared luminescent material applications. Dogan et al. [24] focused on the UC luminescence in $Ho^{3+/}Yb^{3+}$ co-doped tellurite glasses and their temperature sensing properties which are useful for lighting and optical temperature sensing applications. Although there are a lot of studies reported on the up-conversion luminescence and NIR emission on Ho^{3+}/Yb^{3+} co-doped material, the research on Ho^{3+}/Yb^{3+} co-doped glass is still expected to bring interesting luminescent properties in varying crystal environment, heat treatment, phonon energies, dopant concentrations, excitation wavelengths, pump powers, etc.

Based on the above facts, in this work, we have synthesized a new set of Ho^{3+}/Yb^{3+} co-doped tellurite glasses, comprising the composition TeO_2–ZnO–YF_3–NaF. The visible and NIR down conversion emission and intense UC emissions observed in the green and red of Ho^{3+} in the synthesized tellurite glasses with varied amounts of Yb^{3+} are analyzed. In the interim the energy transfer mechanism between Yb^{3+} to Ho^{3+} ions were analyzed.

Experimental details

Glass preparation

A series of glasses with chemical composition (50−*x*−*y*) TeO_2–30ZnO–10YF_3–10NaF–xHo_2O_3–yYb_2O_3 (*x* = 0.5 and *y* = 0.5, 1.0, 3.0 and 5.0 mol%) were prepared by melt-quenching technique. In an agate mortar, rigorously mixed high purity TeO_2 (99.9%), ZnO (99.9%), YF_3 (99.9%), NaF (99.99%), Ho_2O_3 (99.99%) and Yb_2O_3 (99.99%) raw materials. An electrical furnace at air atmosphere is maintained at 1050 °C and 10 g batches of the sample were melted for 30 min. Then the melts were quenched via pouring them into a preheated brass mould which is maintained at 200 °C. For the purpose of avoiding the internal thermal stress-initiated cracking, the glasses were annealed at 300 °C for 4 h, and then brought back to room temperature via natural cooling.

Sample measurements

The density of glass samples was measured using distilled water as an immersion liquid which works based on Archimedes principle. The absorption spectra of the samples were recorded using Perkin Elmer spectrophotometer (Lambda 1050) which operates over the wavelength ranges 300–2000 nm with a spectral resolution of 1 nm. The down conversion emission, excitation, and decay curve analysis were done using Horiba Fluorolog-spectrofluorimeter, that consists of CW and pulsed Xe lamps. The output signals were recorded using a visible photodiode detector (l PPD-850) and by an infrared Hamamatsu photomultiplier. The up-conversion was obtained by Horiba Fluorolog-spectrofluorimeter with laser

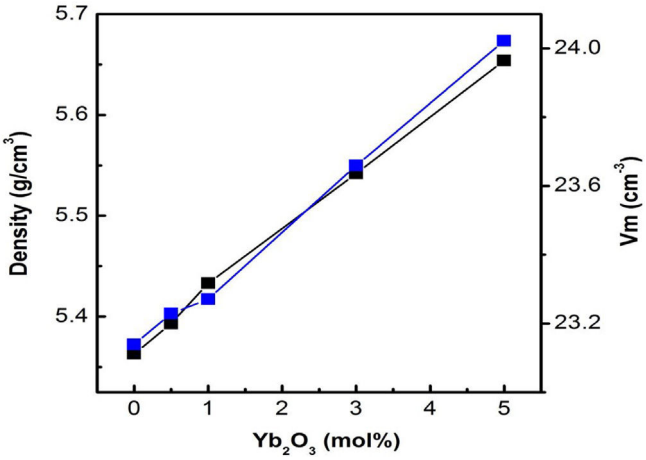

Fig. 1 – The variation of density (g/cm^3) and molar volume (cm^{-3}) as a function of Yb^{3+} ion concentration in oxyfluoro tellurite glasses.

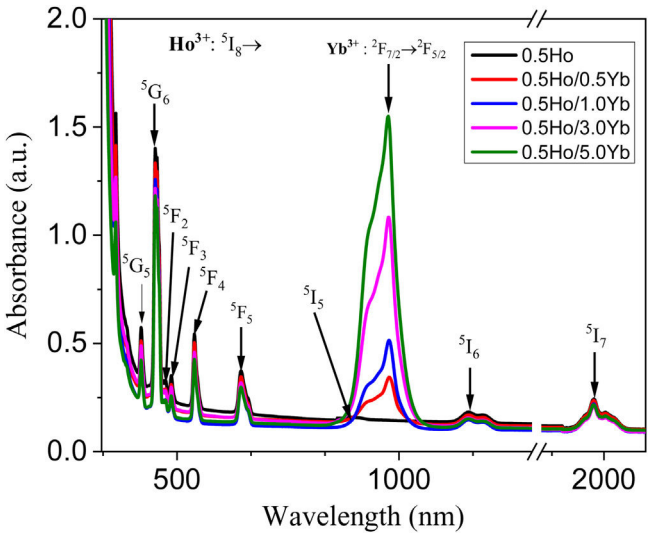

Fig. 2 – Optical absorption spectra of oxyfluoro tellurite glasses doped with Ho^{3+}/Yb^{3+} ions.

diode used as excitation source operating at 980 nm. All the studies were conducted at room temperature.

Results and discussion

Physical properties

The density of the glass matrix influences the bulk properties of the glass samples, such as linear refractive index, etc. [25]. The variation of density (g/cm^3) and molar volume (cm^3/mol) with respect to Yb^{3+} ion concentration in tellurite glasses is studied and is shown in Fig. 1. Both density and molar volume increase with increasing Yb^{3+} concentration; this could be due to the generation of excess non-bridging oxygen (NBO) bonds, that dictates the structure of the respective glass networks, and the replacement of TeO_2 with heavier Yb_2O_3 in the base glass composition [26].

Optical absorption spectra

The optical absorption spectra of Ho^{3+}/Yb^{3+} co-doped tellurite glasses are illustrated in Fig. 2. Absorption peaks at 420, 450, 474, 489 541, 645, 896, 1160 and 1955 nm are referred to the ground level of Ho^{3+} ions ($^5I_8$) to highly excited levels ($^5G_5$, $^5G_6$, $^5F_2$, $^5F_3$, $^5F_4$, $^5F_5$, $^5I_5$, $^5I_6$ and $^5I_7$, respectively) transitions. The Yb^{3+} ions ground level ($^2F_{7/2}$) to the excited level $^2F_{5/2}$ transitions, are referred to the strong absorption peak observed at 978 nm. Therefore, the doping of sensitizer Yb^{3+} ion provided a channel for mid-infrared emission of Ho^{3+}.

Excitation and down-conversion emission

Fig. 3 exhibits the excitation spectra of Ho^{3+}-doped oxyfluoro tellurite glasses. As shown in Fig. 3, the excitation profile for 980 and 1216 nm emission closely resembles its absorption spectrum from 350 to 600 nm. Hence, some of the excitation bands can be readily assigned to $^5I_8 \rightarrow {}^3H_6$ (362 nm), $^5I_8 \rightarrow {}^5G_4$ (388 nm), $^5I_8 \rightarrow {}^5G_5$ (420 nm), $^5I_8 \rightarrow {}^5G_6$, $^5F_1$ (455 nm), $^5I_8 \rightarrow {}^3F_2$ (475 nm), $^5I_8 \rightarrow {}^3F_3$ (487 nm), and $^5I_8 \rightarrow {}^3F_4$ (539 nm) transitions of Ho^{3+} ions, respectively.

The intensity of excitation bands depends on the monitored emission wavelength. For instance, when the spectra were measured at the emission wavelength of 980 nm (Yb^{3+} ion), see Fig. 3(a), the intensity of the bands increased up to 1.0 mol% Yb^{3+} ion contraction. Whereas the intensity of the same bands decreased when monitored at 1216 nm (Ho^{3+} ion), see Fig. 3(b). The energy transfer (ET) from Ho^{3+} to Yb^{3+} ions is responsible for this variation in bands intensity. When the Yb^{3+} ion concentration exceeds 1.0 mol%, the opposite effect is observed. This could be attributed to energy back transfer (EBT) from Yb^{3+} to Ho^{3+} ions via the cross relaxation channels [28], which will discuss below. The ET between Ho^{3+} and Yb^{3+} confirmed by the analysis of down conversion emission spectra, as discussed below.

From Fig. 3, the maximum excitation wavelength is located at 455 nm. Excitation into the strongest $^5I_8 \rightarrow {}^5G_6$, $^5F_1$ transition of Ho^{3+} at 455 nm yields the emission spectrum, as illustrated in Fig. 4(a) in visible (VIS) and Fig. 4(b) in NIR region. The visible spectrum (Fig. 4(a)) consists of the emission bands associated with $^5F_4 \rightarrow {}^5I_8$ (547 nm), $^5F_5 \rightarrow {}^5I_8$ (657 nm), and $^5F_4 \rightarrow {}^5I_7$ (755 nm) of Ho^{3+} ion's transitions. The intensity of these bands decreases with Yb^{3+} concentration due to ET process from Ho^{3+} to Yb^{3+} ions takes place through cross relaxation channels ($^5S_2$, $^5F_4$): Ho^{3+}, $^2F_{7/2}$: $Yb^{3+} \rightarrow {}^5I_6$: Ho^{3+}, $^2F_{5/2}$: Yb^{3+} (in Fig. 5, marked as CR_1) and $^5F_5$: Ho^{3+}, $^2F_{7/2}$: $Yb^{3+} \rightarrow {}^5I_7$: Ho^{3+}, $^2F_{5/2}$: Yb^{3+} (in Fig. 5, marked as CR_2) [28]. Whereas NIR spectra (Fig. 4(b)) consists of emission bands at 980 nm, 1021 nm and 1216 nm, which are referred to the Yb^{3+}: $^2F_{5/2} \rightarrow {}^2F_{7/2}$, Ho^{3+}: $^5F_4$, $^5S_2 \rightarrow {}^5I_6$, and Ho^{3+}: $^5I_6 \rightarrow {}^5I_8$ energy transitions. In contrast to visible emission spectra, although Yb^{3+} ion lack an absorption band in the visible region, the intensity of the 980 nm band increases with Yb^{3+} concentration up to 1.0 mol%, which confirms further that ET takes place from Ho^{3+} to Yb^{3+} ions. However, beyond 1.0 mol% of Yb^{3+} concentration, the intensity drops for 980 nm band and raises for

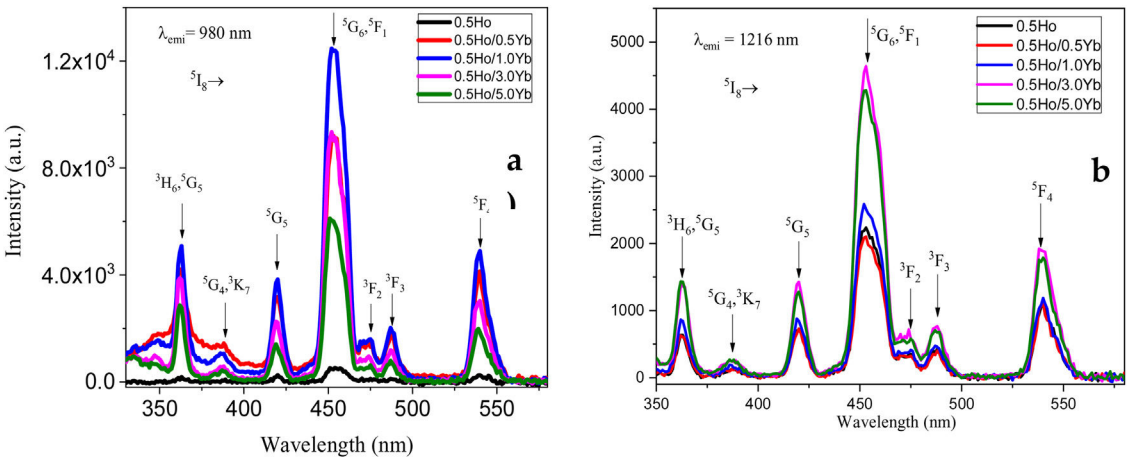

Fig. 3 – Excitation spectra (a) λ_{emi} = 980 nm and (b) λ_{emi} = 1216 nm of oxyfluoro tellurite glasses doped with Ho^{3+}/Yb^{3+} ions.

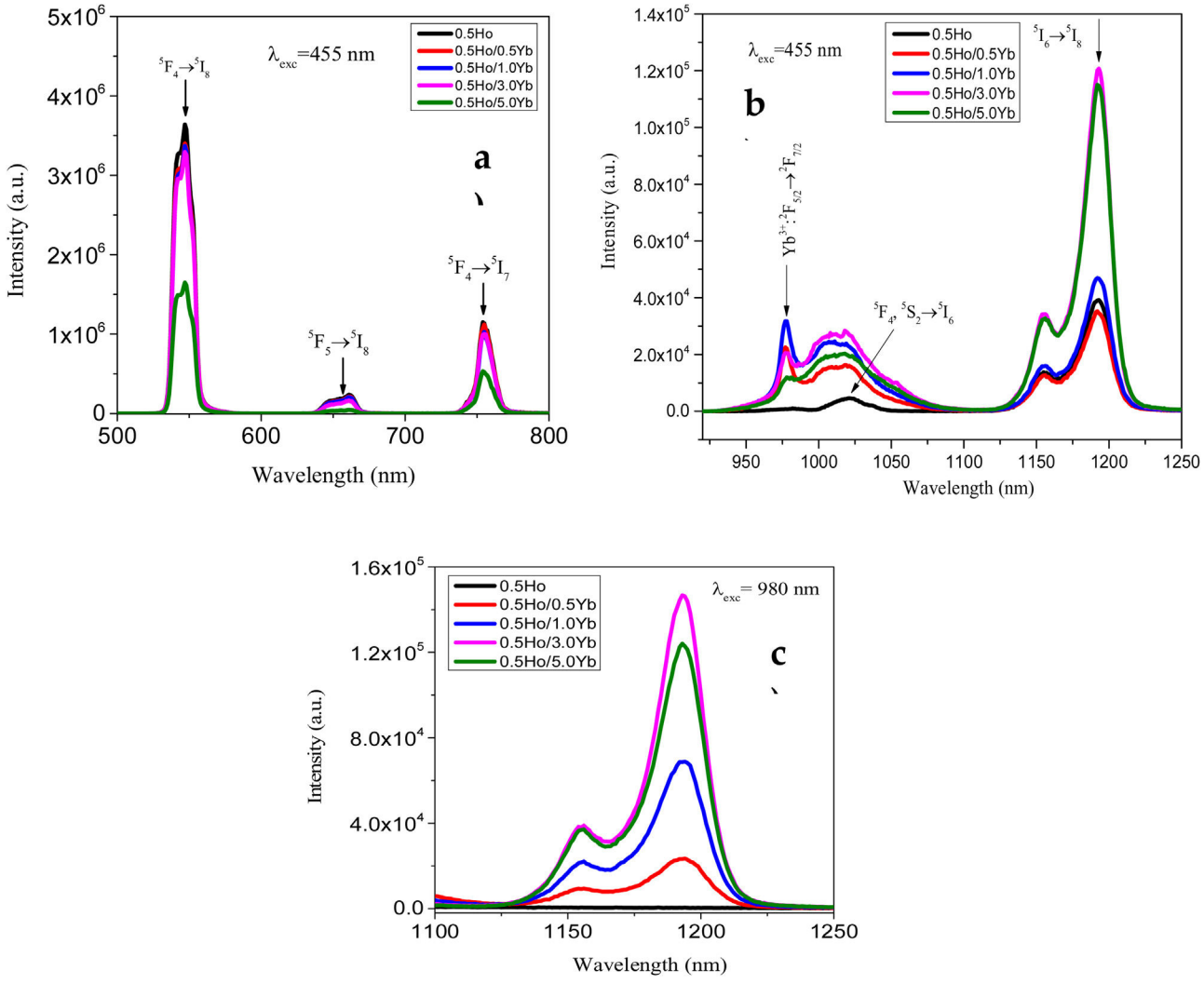

Fig. 4 – Emission spectra in (a) 500–800 nm (λ_{exc} = 455 nm), (b) 900–1250 nm (λ_{exc} = 455 nm), and (c) 1100–1250 nm (λ_{exc} = 980 nm) oxyfluoro tellurite glasses doped with Ho^{3+}/Yb^{3+} ions.

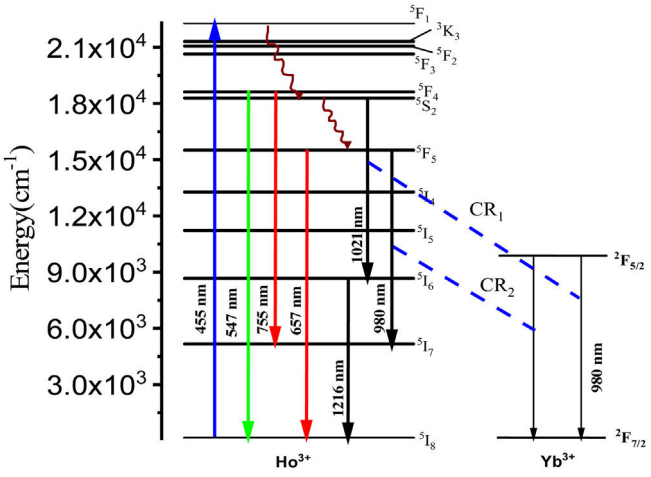

Fig. 5 – Down conversion energy level diagram of oxyfluoro tellurite glasses doped with Ho^{3+}/Yb^{3+} ions.

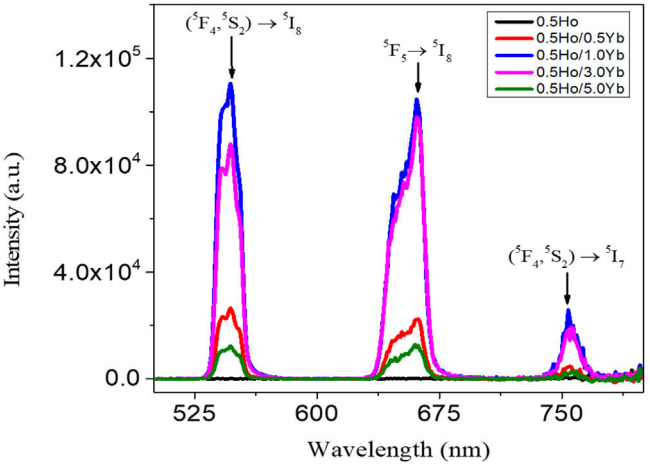

Fig. 6 – Up-conversion emission spectra with different Yb^{3+} concentration in oxyfluoro tellurite glasses doped with Ho^{3+}/Yb^{3+} ions.

1216 nm band have been observed. The change in intensity may be due to EBT from Yb^{3+} to Ho^{3+} ions. Further, despite of change in intensity of 980 nm emission band, change in spectral profile has also been observed with the increase in Yb^{3+} ion concentration. This could be due the fact that luminescence reabsorption by the Yb^{3+} neighboring ions [29]. Fig. 4(c) shows the infrared fluorescence spectra under 980 nm excitation. The emission bands can be readily assigned to $^5I_6 \rightarrow {}^5I_8$ (1201 nm) transition of Ho^{3+} ions.

Up-conversion emissions and energy transfer process

In order to demonstrate the up-conversion emission fluorescence, sensitive fluorescence spectrophotometer adopting at 980 nm pumping laser was used and the up-conversion spectra obtained for the investigated glasses are shown in Fig. 6. The emission bands centering around 546, 661 and 775 nm wavelengths are assigned to the transitions from the Ho^{3+} ion's ($^5F_4$, $^5S_2$) to $^5I_8$, $^5F_5$ to $^5I_8$, and ($^5F_4$, $^5S_2$) to $^5I_7$ levels, respectively. The intensity of these UC emissions gradually raised

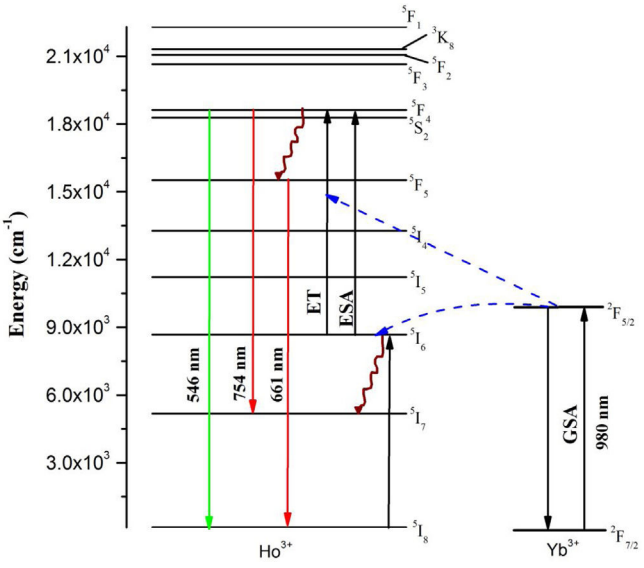

Fig. 7 – Up conversion energy level diagram of Ho^{3+}/Yb^{3+} co-doped oxyfluoro tellurite glasses.

against Yb^{3+} content up to 1.0 mol% and the emission dropped dramatically with further increase in Yb^{3+} ion's concentration. The non-radiative energy transfer process overrides and the resulting concentration quenching effect plays a dominant role in the reduction of UC intensities [27]. The earlier studies reported that the upconversion emission intensity of Ho^{3+}/Yb^{3+} glass centered at 754 nm was very weak compared to the emissions bands centered at 546 nm and 669 nm [22,30–36] and the ratio of peak intensity between 546 nm and 659 nm UC emissions is less than 1, while it is more than 1 in some other studies [37–39]. The value of UC intensity bands centered at 546 nm and 661 nm are maximized when the concentration of Yb^{3+} is 1.0 mol%.

In order to explain the energy transfers from Yb^{3+} to Ho^{3+} ions, the energy diagram given in Fig. 7 is utilized. The studies on power dependency of UC emissions revealed that the intense emissions in green and red is two-photon absorption enabled. The Yb^{3+} ion to Ho^{3+} ion energy transfer populates the Ho^{3+} ion's $^5S_2$ and $^5F_4$ levels which leads to the emission in green and red wavelengths. When excited with near infrared (NIR) photons (980 nm), at first the ground $^2F_{7/2}$ level Yb^{3+} ion gets excited to the $^2F_{5/2}$ level because of its large absorption cross-section. From the excited level of Yb^{3+} ion, the energy transfer takes place to the Ho^{3+} ions which are initially at the ground level, which further gets excited to a $^5I_6$ metastable level through energy transfer (ET). Then, via the excited state absorption (ESA) or the ET, the Ho^{3+} ions existing at the $^5I_6$ excited level reabsorb the incoming NIR wavelength photons to populate the $^5S_2$ ($^5F_4$) energy levels. From there, they return to the ground $^5I_8$ level with the emission of intense radiation in the green region around 546 nm, owing to the energy gap. Also, originated from some non-radiative relaxations, the $^5S_2$ ($^5F_4$) levels of Ho^{3+} ions get transferred to the $^5F_5$ level quickly. Moreover, some possible excited state absorption (ESA) or the ET enables the $^5F_5$ level to get populated, which ultimately

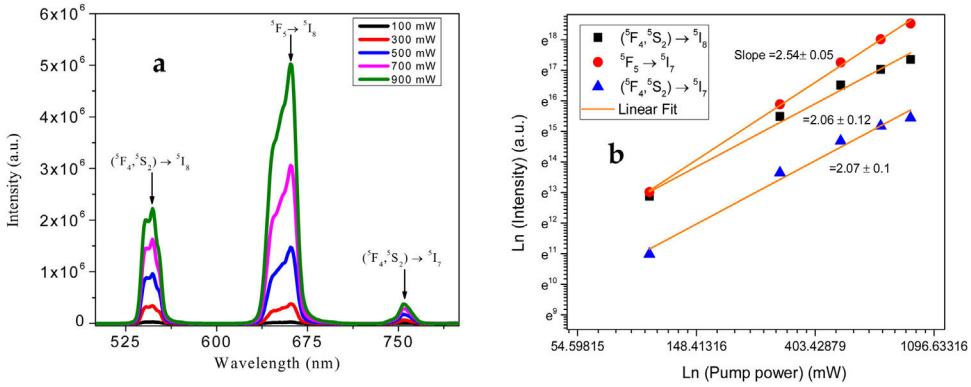

Fig. 8 – (a) Different pump power oxyfluoro tellurite glasses doped with Ho^{3+}/Yb^{3+} ions; (b) dependence integrated up-conversion emission intensities on excitation power in oxyfluoro tellurite glass co-doped with 0.5 mol% Ho^{3+} and 1.0 mol% Yb^{3+} ions.

lead to an intense red-light emission at about 661 nm wavelength [40]. Meantime, the $^5F_4$ ($^5S_2$) level Ho^{3+} ions deplete to the $^5I_7$ metastable state thereby emitting a weak NIR emission at about 754 nm wavelength [41,42].

The UC involves nonlinear optical processes, and hence the UC emissions should be excitation laser intensity dependent. In order to analyze that, the UC emission spectra of the sample under varying pump power scheme is studied, and the obtained graph is given in Fig. 8(a). It shows the UC emission intensities' variation with pump power for all observed transitions. With the increase of pump power, all UC emission intensities shoot up. For these three luminescence peaks, the dependence of integrated up-conversion emission intensities, obtained from Fig. 8(a), is presented in Fig. 8(b). The number of photons (n) take part into the UC process is revealed by linear fit on the intensity-power variation plotted as double logarithmic curve. The slope obtained can give the n value, as it assumed to follow the relation ($I \sim P^n$) [43]. For 0.5 mol% Ho^{3+} and 1.0 mol% Yb^{3+} ions co-doped tellurite glass, the n values of green, red and NIR emissions are 2.07, 2.54 and 2.06, respectively; confirming that three UC emission transitions are populated predominantly by two-photons absorption process. The high n value of red transition ($^5F_5$–$^5I_7$) is indicative of multiphoton cooperative process, in addition to the two-photon absorption process.

Fluorescence decay analysis

In order to unravel the ET process the lifetime measurement was carried out. The time resolved emission spectra (decay curves) of 546 nm ($^5F_4$,$^5S_2$) emission of Ho^{3+} ions by exciting at 455 nm in tellurite glasses are shown in Fig. 9. All decay curves are well fitted with single exponential function. The obtained decay times found to be decreased from 20.23 to 10.44 μs. The reduction in lifetimes with the increase of Yb^{3+} ions concentration warrants the occurrence of strong energy transfer process from Ho^{3+} to Yb^{3+} ions, via cross relaxation channels ($^5S_2$, $^5F_4$): Ho^{3+}, $^2F_{7/2}$: $Yb^{3+} \rightarrow {}^5I_6$: Ho^{3+}, $^2F_{5/2}$: Yb^{3+} and $^5F_5$: Ho^{3+}, $^2F_{7/2}$: $Yb^{3+} \rightarrow {}^5I_7$: Ho^{3+}, $^2F_{5/2}$: Yb^{3+} (see in Fig. 6) [14].

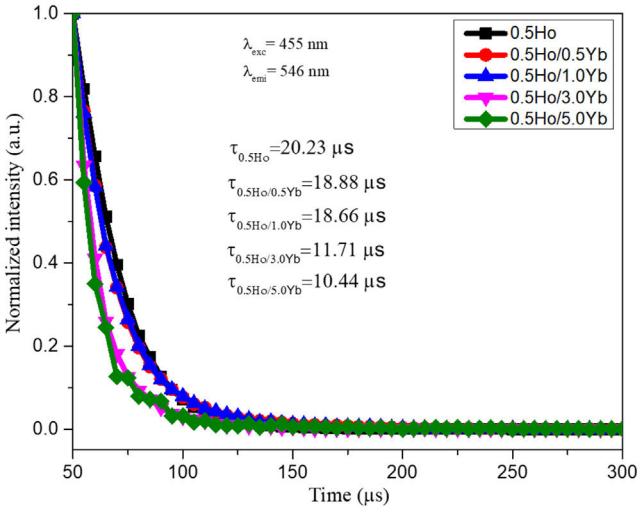

Fig. 9 – Decay curve of the 546 nm emission (Ho^{3+}: $^5F_4$ level) for oxyfluoro tellurite glass co-doped with Ho^{3+}/Yb^{3+} ions.

Conclusion

In this report, a series of glasses with chemical composition (50−x−y) TeO_2–30ZnO–10YF_3–10NaF–xHo_2O_3–yYb_2O_3 (x = 0.5 and y = 0.5, 1.0, 3.0 and 5.0 mol%) is prepared by melt-quenching technique. The absorption spectra, excitation, visible emission, up-conversion emission spectra and decay time measurements were characterized. Under the 980 nm laser excitation, the sample exhibited intense green (546 nm), red (661 nm), and NIR emissions (754 nm). The UC emission intensity variation study with respect to excitation pump power indicated that the two-photon absorption mechanism based on the energy transfer from Yb^{3+} to Ho^{3+} was the source of the Ho^{3+} population at $^5F_4$ ($^5S_2$) and $^5F_5$ levels. With the increase of Yb^{3+} ions concentration, the green and red up-conversion emission intensities show significant enhancement. Hence, the present results indicate that the newly synthesized Ho^{3+}/Yb^{3+}-co-doped TeO_2–ZnO–YF_3–NaF

glass with intense up-conversion emissions in the green and red wavelengths could be a promising material that will find applications in the visible-band fiber lasers and photonics.

Funding

This research was funded by Kuwait Foundation for the Advancement of Sciences, Kuwait, grant number PR18-14SP-11.

Acknowledgments

S.K. acknowledges Kuwait Foundation for the Advancement of Sciences (KFAS) for the research fund (PR18-14SP-11). This work is a part of the activities of the FunGlass project. R.D. acknowledges the funding from the European Union Horizon 2020 research and innovation program under grant agreement No. 739566 and S.E. acknowledges SERB, India for NPDF No. PDF/2020/002494.

REFERENCES

[1] G. Blasse, B.C. Grabmaier, Luminescent Material, 1st ed., Springer-Verlag, Berlin, Germany, 1994, pp. 33–70.
[2] A. Shalav, B.S. Richards, M.A. Green, Luminescent layers for enhanced silicon solar cell performance: up-conversion, Sol. Energy Mater. Sol. Cells 91 (2007) 829–842.
[3] J.H. Zang, J. Su, Z.H. Li, R.X. Yan, Y.D. Li, Synthesis and upconversion luminescence of hexagonal-phase $NaYF_4$:Yb, Er^{3+} phosphors of controlled size and morphology, Adv. Mater. 17 (2005) 2119–2123.
[4] R. Stepien, R. Buczynski, D. Pysz, I. Kujawa, A. Filipkowski, M. Mirkowska, R. Diduszko, Development of thermally stable tellurite glasses designed for fabrication of microstructured optical fibers, J. Non-Cryst. Solids 357 (2011) 873–883.
[5] J. Jakutis, L. Gomes, C.T. Amancio, L. Kassab, J.R. Martinelli, N.U. Wetter, Increased Er^{3+} upconversion in tellurite fibers and glasses by co-doping with Yb^{3+}, Opt. Mater. 33 (2010) 107–111.
[6] S. Balaji, A.K. Mandal, K. Annapurna, Energy transfer based NIR to visible upconversion: enhanced red luminescence from Yb^{3+}/Ho^{3+} co-doped tellurite glass, Opt. Mater. 34 (2012) 1930–1934.
[7] P. Babu, I.R. Martin, K.V. Krishnaiah, H.J. Seo, V. Venkatramu, C.K. Jayasankar, V. Lavin, Photon avalanche upconversion in Ho^{3+}–Yb^{3+} co-doped transparent oxyfluoride glass–ceramics, Chem. Phys. Lett. 600 (2014) 34–37.
[8] K.V. Krishnaiah, R. Rajeswari, K.U. Kumar, S.S. Babu, I.R. Martin, C.K. Jayasankar, Spectroscopy and radiation trapping of Yb^{3+} ions in lead phosphate glasses, J. Quant. Spectrosc. Radiat. Transfer 140 (2014) 37–47.
[9] K. Biswas, A.D. Sontakke, R. Sen, K. Annapurna, Enhanced 2 μm broad-band emission and NIR to visible frequency up-conversion from Ho^{3+}/Yb^{3+} co-doped Bi_2O_3–GeO_2–ZnO glasses, Spectrochim. Acta A 112 (2013) 301–308.
[10] S. Bose, D. Misra, R. Debnath, Ho^{3+} ion in a (Ba, La)-tellurite glass: strong ~2.0 μm NIR emission and Yb^{3+} aided efficient NIR to vis upconversion, Opt. Mater. 36 (2013) 221–227.
[11] H. Li, H. Hao, S. Jin, W. Guo, X. Hu, H. Hou, G. Zhang, S. Yan, W. Gao, G. Liu, Synthesis and luminescence properties of Ho^{3+}/Yb^{3+} co-doped bismuth tungstate nanopowder, Mater. Res. Bull. 89 (2017) 51–56.
[12] D. Przybylska, A. Ekner-Grzyb, B.F. Grzeskowiak, T. Grzyb, Upconverting SrF2 nanoparticles doped with Yb^{3+}/Ho^{3+} Yb^{3+}/Er^{3+} and Yb^{3+}/Tm^{3+} ions – optimisation of synthesis method, structural, spectroscopic and cytotoxicity studies, Sci. Rep. 9 (2019) 8669.
[13] S. Balaji, A.D. Sontakke, R. Sen, A. Kalyandurg, Efficient 2.0 μm emission from Ho^{3+} doped tellurite glass sensitized by Yb^{3+} ions: Judd–Ofelt analysis and energy transfer mechanism, Opt. Mater. Exp. 1 (2011) 2.
[14] H. Jianli, Z. Zhiguang, Z. Huan, L. Aoxiang, Intense red fluorescence from Ho/Yb codoped tellurite glasses, J. Non-Cryst. Solids 383 (2014) 157–160.
[15] M. Seshadri, L.C. Barbosa, C.M.B. Cordeiro, M. Radha, F.A. Sigoli, Y.C. Ratnakaram, Study of optical absorption, visible emission and NIR–vis luminescence spectra of Tm^{3+}/Yb^{3+}, Ho^{3+}/Yb^{3+} and Tm^{3+}/Ho^{3+}/Yb^{3+} doped tellurite glasses, J. Lumin. 166 (2015) 8–16.
[16] L. Yu, C. Muzhi, C. Ruijie, T. Ying, H. Feifei, X. Shiqing, Z. Junjie, Enhanced effect of Er^{3+} ions on 2.0 and 2.85 μm emission of Ho^{3+}/Yb^{3+} doped germanate–tellurite glass, Opt. Mater. 57 (2016) 60252–60262.
[17] Z. Wang, F. Huang, B. Li, Y. Li, Y. Tian, S. Xu, Enhanced luminescence properties of Ho/Yb ions regulated by the nanocrystalline environment and phonon energy in silicate glasses, J. Lumin. 219 (2020) 116949.
[18] P.X. Le, N.M. Ty, J. Qiu, D. Zhou, H. Kim Dan, Enhanced upconversion and near-infrared emissions of co-doped Ho^{3+}/Yb^{3+} in TeO_2–ZnO–Na_2CO_3–La_2O_3 tellurite glasses, Opt. Mater. Exp. 9 (2019) 3998.
[19] K. Suresh, C.K. Jayasankar, Conversion of blue-green photon into NIR photons in Ho^{3+}/Yb^{3+} co-doped zinc tellurite glasses, J. Alloys Compd. 788 (2019) 1048–1055.
[20] Z. Yarui, S. Xinjie, Z. Minghan, S. Xiue, L. Jun, Y. Gaobo, S. Hanru, Z. Yaxun, 2.0 μm band emission enhancement and energy transfer in Ho^{3+}/Yb^{3+}/Er^{3+} tri-doped tellurite glasses, J. Lumin. 210 (2019) 28–37.
[21] H. Guangning, Z. Chaomin, F. Wenbin, L. Guishun, X. Jinan, P. Yunxia, Broadband mid-infrared 2.0 μm and 4.1 μm emission in Ho^{3+}/Yb^{3+} co-doped tellurite–germanate glasses, J. Lumin. 217 (2020) 1166769.
[22] A. Mohd, K.M. Deepak, K.R. Vineet, K. Singh, Luminescence and Judd–Ofelt study of Ho^{3+}/Ho^{3+}–Yb^{3+} doped/codoped lead tellurite glasses for multifunctional applications, J. Lumin. 239 (2021) 118319.
[23] Y. Chao, L. Zhangwen, P. Yunxia, M. Xuelong, Z. Chaomin, Up-conversion and 2 μm mid-infrared emission effective enhancements in Ho^{3+}/Yb^{3+} co-doped tellurite glass, Optik 242 (2021) 167262.
[24] D. Anil, E. Murat, E. Kadir, E. Gonul, Upconversion luminescence and temperature sensing characteristics of Ho^{3+}/Yb^{3+} co-doped tellurite glasses, J. Non-Cryst. Solids 571 (2021) 121055.
[25] D. Kumar, S.M. Rao, S. Pal Singh, Structural, optical and thermoluminescence study of Dy^{3+} ion doped sodium strontium borate glass, J. Non-Cryst. Solids 464 (2017) 51–55.
[26] F.A. Moustafa, M. Abdel-Baki, A.M. Fayad, F. El-Diasty, Role of mixed valence effect and orbital hybridization on molar volume of heavy metal glass for ionic conduction pathways augmentation, Am. J. Mater. Sci. 4 (2014) 119–126.
[27] M. Pollnau, D.R. Gamelin, S.R. Lüthi, H.U. Güdel, M.P. Hehlen, Power dependence of upconversion luminescence in lanthanide and transition-metal-ion systems, Phys. Rev. B 61 (2000) 3337–3346.
[28] Y. Pei, S. An, C. Zhuang, D. Sun, X. Li, J. Zhang, Yb^{3+}-concentration-dependent upconversion luminescence of Ho^{3+}–Yb^{3+}, co-doped $La_{9.31}(Si_{1.04}O_4)_6O_2$ for optical thermometer, J. Lumin. 250 (2022) 119073–119079.

[29] K. Venkata Krishnaiah, E. Soares de Lima Filho, Y. Ledemi, G. Nemova, Y. Messaddeq, R. Kashyap, Development of ytterbium-doped oxyfluoride glasses for laser cooling applications, Sci. Rep. 6 (2016) 21905.
[30] Y. Fu, W.H. Cao, Y.X. Peng, X. Luo, M.M. Xing, The upconversion luminescence properties of the Yb^{3+}–Ho^{3+} system in nanocrystalline Y_2O_2S, J. Mater. Sci. 45 (2010) 6556–6561.
[31] X. Wang, X.P. Li, S. Xu, L.H. Cheng, J.S. Sun, J.S. Zhang, B.J. Chen, Can temperature be accurately sensed by red-green emission ratio in $YNbO_4$: Ho^{3+}/Yb^{3+} phosphor under 980 nm excitation, J. Alloys Compd. 754 (2018) 222–226.
[32] X.Y. Wang, H. Lin, D.H. Yang, L. Lin, E.Y.B. Pun, Optical transitions and upconversion fluorescence in Ho^{3+}/Yb^{3+} doped bismuth tellurite glasses, J. Appl. Phys. 101 (2007) 113535.
[33] Y. Gao, Y.B. Hu, D.C. Zhou, J.B. Qiu, Upconversion luminescence properties of $NaYF_4$ nanocrystals precipitated Nd^{3+}/Yb^{3+}/Ho^{3+} tri-doped oxyfluoride glass–ceramics, J. Nanosci. Nanotechnol. 16 (2016) 3744–3748.
[34] L. Feng, Q. Su, Y. Li, C.R. Zheng, C. Wang, H. Li, Compositional thermal effect on upconversion luminescence of Ho^{3+}/Yb^{3+} co-doped oxyfluoride glasses, Spectrochim. Acta Part A 73 (2009) 41–43.
[35] Z.F. Shan, D.Q. Chen, Y.L. Yu, P. Huang, F.Y. Weng, H. Lin, Y.S. Wang, Upconversion luminescence of Ho^{3+} sensitized by Yb^{3+} in transparent glass ceramic embedding BaYF5 nanocrystals, Mater. Res. Bull. 45 (2010) 1017–1020.
[36] L.L. Han, H.H. Yao, S.L. Miao, S. Wang, J. Zhao, T. Sun, C. Guo, Z.P. Ci, C.W. Wang, Morphology controllable synthesis and upconversion luminescence of $Gd_4O_3F_6$: Ho^{3+}, Yb^{3+} for temperature sensing, J. Lumin. 197 (2018) 360–369.
[37] B.R. Li, X. Zhao, E.Y. Pun, B.H. Lin, Upconversion photon quantification of Ho^{3+} in highly transparent fluorotellurite glasses, Opt. Laser Technol. 107 (2018) 8–14.
[38] N.K. Giri, S.B. Rai, A. Rai, Intense green and red upconversion emissions from Ho^{3+} in presence of Yb^{3+} in Li: TeO_2 glass, Spectrochim. Acta Part A 74 (2009) 1115–1119.
[39] C.H. Niu, L.W. Li, X.Y. Li, Y. Lv, X.P. Lang, Upconversion photoluminescence properties of Ho^{3+}/Yb^{3+} co-doped $YNbO_4$ powder, Opt. Mater. 75 (2018) 68–73.
[40] Z. Chen, W. Cui, S. Kang, H. Zhang, G. Dong, C. Jiang, S. Zhou, J. Qiu, Fast–slow red upconversion fluorescence modulation from Ho^{3+}-doped glass ceramics upon two-wavelength excitation, Adv. Opt. Mater. 5 (2016) 1600554.
[41] C. Joshi, K. Kumar, S.B. Rai, Structural, thermal, and optical properties of Pr^{3+}/Yb^{3+} co-doped oxyhalide tellurite glasses and its nano-crystalline parts, Opt. Commun. 284 (2011) 4584–4587.
[42] Y. Yu, Y.D. Zheng, F. Qin, Z.M. Cheng, C.B. Zheng, Z.G. Zhang, W.W. Cao, Experimental investigation on the upconversion mechanism of 754 nm NIR luminescence of Ho^{3+}/Yb^{3+}:Y_2O_3, Gd_2O_3 under 976 nm diode laser excitation, J. Lumin. 131 (2011) 190–193.
[43] J.F. Suyver, A. Aebischer, S. García-Revilla, P. Gerner, H.U. Güdel, Anomalous power dependence of sensitized upconversion luminescence, Phys. Rev. B: Condens. Matter Mater. Phys. 71 (2005) 125123.